



Cyclic loading effects and stability assessment of trees and stumps used as anchors in cable yarding operations

Luca Marchi¹ · Omar Mologni² · Ken Byrne² · Stefano Grigolato^{1,3} · Dominik Roeser²

Received: 12 March 2024 / Revised: 15 May 2024 / Accepted: 18 June 2024 / Published online: 5 July 2024
© The Author(s) 2024

Abstract

Swing yarders in running skyline configuration using either grapples or chokers represent the most common configuration for cable yarding in coastal British Columbia. In this context, whole-tree logging and short work cycles lead to heavy and repeated loads applied to the trees and stumps when used as anchors for the rigging cables. Moreover, increased harvesting of second-growth forest stands leads to the unavailability of large and safe trees, thus introducing new challenges to identify suitable anchors and potentially increases safety risks of cable yarding operations.

The present study aimed to collect evidence of the mechanical response provided by anchors for typical cable yarders used in second-growth harvesting in coastal British Columbia, and test the suitability of innovative techniques for the stability assessment based on the relationship between the anchor root-plate rotations and the related applied tensile forces. A conspicuous dataset could be derived from all the surveys, storing anchor rotations from a total of 1522 work cycles of which 1224 work cycles included also tensions measurements. The methodological approach was proven effective for monitoring different rigging configurations giving proof that repeated loading affects the stability of a tree/stump which can rapidly change over few hours of active yarding operations. Acquired data proved also that comparing theoretical failure limits with anchor rotations could be a valid approach however a considerable amount of species-specific data from tree pulling tests is required.

Keywords Cable logging · Forest operations · Tree stability · Safety assessment · MEMS sensors

Abbreviations

DBH	Diameter at breast height
F	Tensile force applied to an anchor
$F_{i,max}$	Maximum value of cable tensile force recorded within a work cycle
F_{max}	Maximum value of cable tensile force measured

H	Height of the tree or stump
ID	Damage index, slope of the regression model of $K_i / K_{i,max}$ over n
K_i	Rotational stiffness calculated within a work cycle
$K_{i,max}$	Maximum value of K_i over all work cycles
M	Moment applied to the anchor
M_{peak}	Peak moment corresponding to tree overturning
PMH	Productive time
R_x, R_y	Root-plate rotations measured on the local axes of the inclinometer
R_0, R_{90}	Root-plate rotations parallel and perpendicular to the direction of the pulling force
$R_{i,max}$	Maximum value of the root-plate rotation within a work cycle
R_{max}	Maximum value of the root-plate rotation measured on an anchor over all work cycles
R_{Mpeak}	Root-plate rotation corresponding to M_{peak}
S_R	Safety factor on rotations, equal to $R_{max} /$

Communicated by Eric R. Labelle.

✉ Luca Marchi
luca.marchi@unipd.it

¹ Department of Land Environment Agriculture and Forestry, Università degli Studi di Padova, Viale dell'Università 16, Legnaro, PD 35020, Italy

² Department of Forest Resources Management, Faculty of Forestry, The University of British Columbia, 2424 Main Mall, Vancouver, BC V6T 1Z4, Canada

³ Department of Forest and Wood Science, Stellenbosch University, Paul Sauer Building, Bosman Street, Stellenbosch 7599, South Africa

S_M	$R_{M_{peak,th}}$ Safety factor on moments, equal to $M_{max} / M_{peak,th}$
a_i	Intercept of K_i
n	Cycle number
r_i^2	Coefficient of determination of K_i
ΔR	Azimuthal increment to correct R_x and R_y

Introduction

Logging operations in mountainous areas are increasingly relying on recently introduced ground-based winch-assist technologies because of their potential safety and economic benefits (Heinimann 1999; Visser and Stampfer 2015; Holzfeind et al. 2020). The employment of ground-based machines, however, is limited by accessibility, excessive ground slope, ground roughness, and soil conditions (Amishev et al. 2009). For this reason, cable yarding still represents the preferred harvest system for many steep slope logging operations.

Independently on the rigging configuration, stable anchors are required to secure and safely operate cable yarders. Artificial anchors (e.g., pieces of equipment, dead-man anchors, etc.) allow a relatively reliable estimation of the anchoring capacity (Leshchinsky et al. 2016; Belart et al. 2020), but their use is frequently limited to accessible ground and machine availability. For this reason, the yarding crews must frequently rely on trees and/or stumps (hereafter named natural anchors) to set up cable roads and secure their machines.

Failures of natural anchors, together with excessive cable tensile forces, are indeed primary safety concerns in all cable-supported harvesting systems (Tsioras et al. 2011). Various publications have recently focused on assessing these safety concerns in cable yarding, both in terms of cable tensile forces (Harrill and Visser 2016; Mologni et al. 2019, 2021a, b) as well as anchor stability of various cable yarding operations (e.g., Mancuso et al. 2018; Marchi et al. 2019, 2021). While cable tensile forces can be effectively monitored and eventually controlled, anchor loading capacity is still largely overlooked because of the missing availability of operational solutions for their actual assessment and monitoring, and still too little is known about the behavior of trees and stumps used to anchor cables (Cavalli 2012; Marchi et al. 2018). In several geographical contexts, the challenge of selecting suitable natural anchors and the related safety concerns is also increasing. This is particularly true in some regions of the Pacific Northwest of the United States and Western Canada, where logging operations are transitioning to a major component of second-growth

stands, typically characterized by much smaller tree size compared to local old growth stands (Belart et al. 2020).

The empirical rules formulated by Pestal (1961) still generally represent the current methods to estimate the load capacity of natural anchors. Based on these rules the maximum load bearing capacity of a natural anchor is set to be proportional to the squared diameter at breast height (DBH). As it is well recognised by various best-practice guidelines and safety regulations, however, even if DBH is a straightforward allometric parameter, multiple other variables might affect anchor stability, including for example ground conditions, soil moisture, tree or stump health, and many others (Liley 1983; Samset 1985; Work Safe 2006; OR-OSHA 2010; Safe Work Australia 2013). Relevant pioneering studies were conducted in the past to assess the capacity of natural anchors in withstanding loads originating from cable logging operations, either for standing trees (Pyles 1987; Pyles et al. 1991) or stumps (Stoupa 1984; Toupin et al. 1985; Pyles and Stoupa 1987; Parker 2001). Additional works were conducted also to assess a stump loading capacity when used as road fill retainers for temporary forest roads (Parker 2001, 2002). A detailed review of those work is available in Marchi et al. (2018).

To overcome the shortcomings in effective evaluation methods for anchor movements and overall stability, Marchi et al. (2020) recently presented an assessment method based on the comparison of the anchor root-plate rotations with the applied tensile forces and related moments using low-cost inclinometers and accelerometers. The method was successfully tested in the assessment of nine skyline anchors employed by European-designed tower yarders in standing skyline configurations. The current work aimed to improve this newly introduced methodological approach for the evaluation of the anchor loading capacity with the inclusion of a meticulous cyclic response analysis aimed to derive possible degradation of the elasticity caused by the damages at the root-soil plate (Yang et al. 2020). Improvements included the semi-automatic calculation of the base mechanical stiffness, the analysis of its time-dependency throughout the regression of average stiffness per work cycle over the total number of work cycles, and the identification of a related damage index. The study also aimed to extend the collection of real evidence of the mechanical response of natural anchors stability in cable yarding operations, with a focus on swing yarders adopted in Western Canada and evaluate their response in comparison with theoretical limits known from the literature for the same species growing in similar conditions.

Table 1 Site and stand data related to the three observed blocks

Site	Block 1	Block 2	Block 3
Location	Maple Ridge, B.C.	Maple Ridge, B.C.	Alberni-Clayoquot, B.C.
Harvested area (ha)	16.5	1.9	31.1
Harvested volume (m ³)	9317	1900	22 392
Stand age (years)	70	130	68
Species composition (%)	46 ¹ ; 36 ² ; 16 ³ ; 2 ⁴	63 ¹ ; 30 ² ; 5 ³ ; 2 ⁴	84 ¹ ; 2 ² ; 9 ³ ; 5 ⁴

Species composition expressed as percentage of stand volume. ¹Hw: western hemlock; ²Cw: western red cedar; ³Fd: Douglas-fir; ⁴Others

Materials and methods

Study sites

The study focused on ordinary cable yarding operations in three different cutblocks located in coastal British Columbia (BC), Canada. A preliminary field trial to test equipment and data collection protocol limited to the monitoring of anchor movements was conducted in late January 2021, near Maple Ridge, at the Malcolm Knapp Research Forest, 60 km east of Vancouver (hereafter Block 1). Further data, integrated with high-frequency cable tensile force monitoring, was collected between February and March 2021 in two other cut blocks: one in Maple Ridge, in a similar area of Block 1, and one on Vancouver Island, in the Alberni-Clayoquot Regional District, 30 km north of Bamfield (from now on

Block 2 and Block 3, respectively). The study investigated cable yarding operations in second-growth forest stands with ages ranging from 68 to 130 years. The stands were dominated by Western hemlock (*Tsuga heterophylla*), representing between 46% and 84% of the stand volume, Western red cedar (*Thuja plicata*), and Douglas-fir (*Pseudotsuga menziesii*) (Table 1). The soils in the study area had a fresh soil moisture regime and a medium to rich soil nutrient regime.

The cutblocks were hand felled and yarded by swing yarders in running skyline configuration. Blocks 1 and 2 were yarded by a 1980 Washington Logging Equipment 78 Super SL, re-manufactured in 2020, using both a grapple carriage and a carriage with chokers (Fig. 1). This machine had a total mass of 44.5 tonnes, an engine power of 230 kW, and it was equipped with 19-mm swaged haulback line (skyline), 15.9-mm swaged mainline and slackpuller, and three 22.2-mm guylines. Block 3 was yarded by a 1989 Madill 122 equipped with a grapple carriage (Fig. 2). This machine had a total mass of 53 tonnes and was equipped with a 340-kW engine, 22.2-mm swaged haulback line (skyline), mainline, and slackpuller, and two 28.6-mm guylines.

A total of 15 cable roads were observed during the study (Fig. 3), all in uphill configuration with except of the two cable roads monitored Block 1. The cable roads ranged from 102 to 181 m in horizontal length and from 23 to 51% in slope of the geometric chord (Table 1). In all the three cut blocks, the yarder was located in a single central landing

Fig. 1 WLE 78 Super SL at landing of Block 2 **a** and carriage used **b**



(a)



(b)

Fig. 2 Swing yarder Madill 122 at the landing of Block 3 **a** and grapple carriage used **b**



(a)



(b)

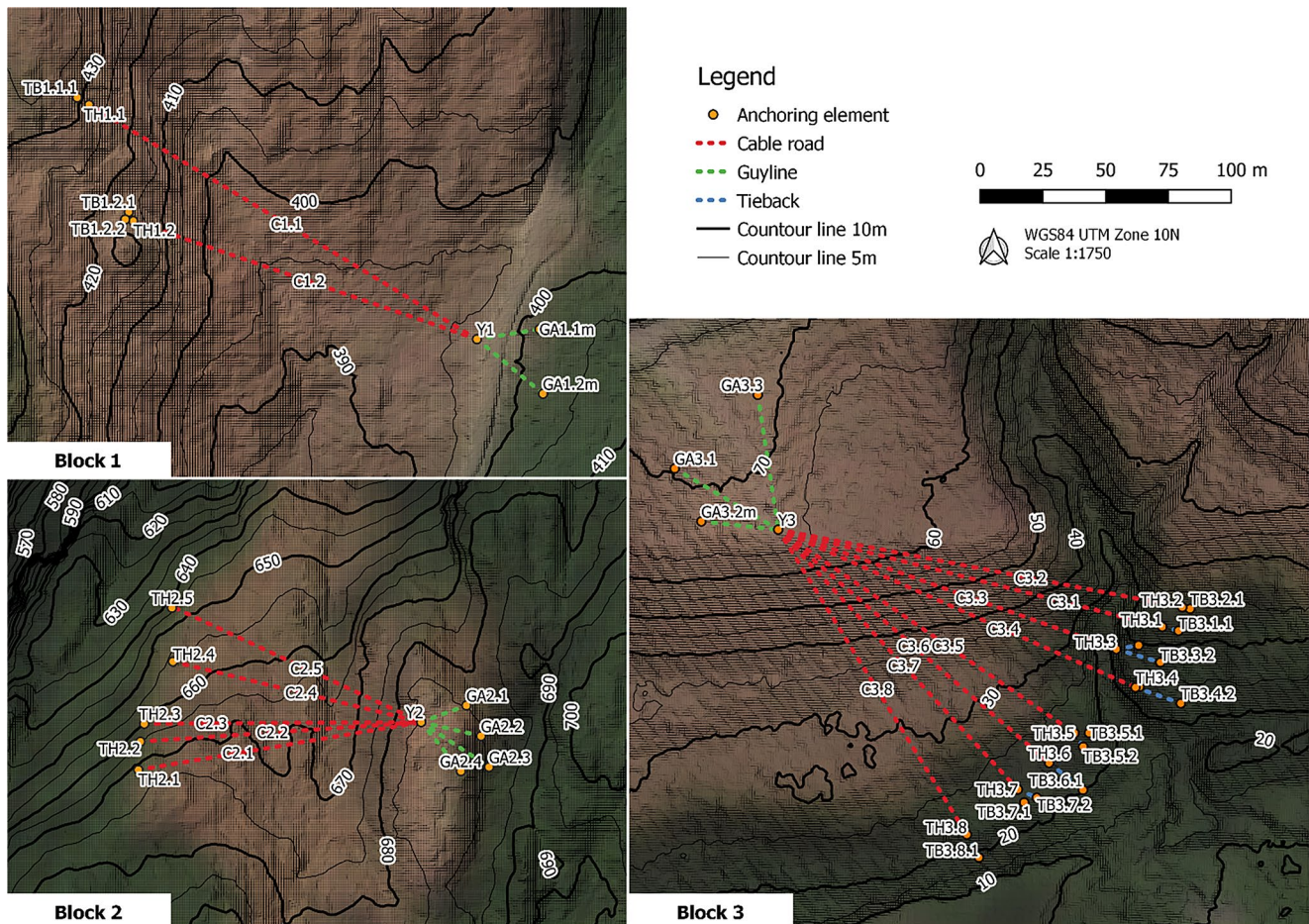


Fig. 3 Cable roads and rigging configurations

position, and the cable roads were progressively moved. Pieces of equipment were used for guyline anchors in Block 1 and, partially, in Block 3. All the other anchors were either trees or stumps (i.e., natural anchors) of various tree species.

Direct field monitoring involved a total of 26 natural anchors (Table 2) including 15 tailholds (here defined as the skyline anchor - either a tree or a stump - used to secure haulback line blocks); eight tiebacks (here defined as trees/stumps used to support tailholds that do not appear to be strong enough through the use of twistors or slings), and three guyline anchors (here defined as the anchor - by regulation a stump, but seldomly a tree - used to secure the yarder's guylines). Tailholds included nine trees with diameter at breast height (DBH) ranging from 38 to 92 cm and six freshly-cut stumps with DBH estimated by taper functions (Omule and Kozak 1989) ranging from 55 to 64 cm. Ten of these tailholds (all those in Block 1 and 3) were supported by one or more tiebacks. The root-plate rotations of tiebacks supporting seven of these tailholds were also monitored (including the monitoring of two tiebacks supporting tailhold TH1.2). These tiebacks included trees with DBH ranging from 21 to 63 cm, and stumps with estimated DBH

from 29 to 55 cm. Guyline anchors included two stumps with estimated DBH of 81 and 94 cm, respectively, and a 107-cm DBH tree. Seventeen out of 26 natural anchors were Western hemlock, while the others were mostly Western red cedar or Douglas fir (Table 2).

Data collection and preliminary data analysis

Cable road layouts and the location of cable yarders, guyline anchors, and tailholds were collected using a GNSS Garmin GPSMAP® 64sx. Relative distance and azimuth measurements from tailholds were used for locating the tiebacks, when needed. Positioning of the various anchor types was also verified by high-resolution Planet satellite images. The integration of this spatial information with Lidar-based digital elevation models provided length and slope of the observed cable roads. Multiple cameras (including in-cab cameras) were used to record the cable yarding operations and facilitate a time study to detect work cycles and productive time including delays up to 15 min (PMH₁₅).

Root-plate rotations of the anchor trees/stumps were monitored by means of micro-electro-mechanical systems

Table 2 Characteristics of the cable roads and monitored anchors

Block	Cable road ID	Horizontal line (m)	Slope (%) ¹	Anchor ID	Anchor type	Tree/ Stump	DBH (cm)	Height (m)	Species ²
1	C1.1	181	24	TH1.1	Tailhold	Stump	55	0.6	Hw
				TB1.1.1	Tieback	Stump	40	0.5	Hw
	C1.2	145	23	TH1.2	Tailhold	Stump	58	0.5	Hw
				TB1.2.1	Tieback	Stump (dead)	55	0.6	Fd
				TB1.2.2	Tieback	Stump	29	0.4	Hw
2	C2.1	114	25	TH2.1	Tailhold	Stump	58	0.6	Cw
	C2.2	112	31	TH2.2	Tailhold	Tree	78	35.5	Fd
	C2.3	110	35	TH2.3	Tailhold	Tree	76	34	Fd
	C2.4	102	42	TH2.4	Tailhold	Stump	60	0.4	Hw
	C2.5	108	51	TH2.5	Tailhold	Tree	71	38	Hw
	C2.1 to C2.5 ³			GA2.3	Guyline anchor	Tree	107	31.5	Fd
3	C3.1	158	22	TH3.1	Tailhold	Tree	38	30	Hw
	C3.2	164	21	TH3.2	Tailhold	Stump	64	1	Hw
				TB3.2.1	Tieback	Tree	27+21	30.0+30.0	Hw+Hw
	C3.3	143	31	TH3.3	Tailhold	Tree	48	38	Hw
				TB3.3.1	Tieback	Tree	54	38	Fd
	C3.4	156	28	TH3.4	Tailhold	Tree	56	38	Hw
				TB3.4.1	Tieback	Tree	63	42	Hw
	C3.5	143	30	TH3.5	Tailhold	Stump	64	1.2	Hw
				TB3.5.1	Tieback	Tree	33	28	Hw
	C3.6	142	31	TH3.6	Tailhold	Tree	61	38	Hw
	C3.7	141	31	TH3.7	Tailhold	Tree	51	33.5	Hw
				TB3.7.1	Tieback	Tree	42	30.5	Hw
	C3.8	143	31	TH3.8	Tailhold	Tree	92	36	Ss
C3.1 to C3.5 ²			GA3.1	Guyline anchor	Stump	94	1.2	Cw	
C3.6 to C3.8 ²			GA3.3	Guyline anchor	Stump	81	0.5	Cw	

¹Slope of the chord line connecting tower yarded to tailhold

²Cw: Western red cedar, Fd: Douglas fir, Hw: Western hemlock, Ss: Sitka spruce (*Picea sitchensis*)

³Multiple cable roads used the same guyline anchor

(MEMS) inclinometers and accelerometers installed at the base of the anchors and aligned with the expected cable pulling forces. The movements of tailholds were recorded using a biaxial inclinometer (Beanair GmbH, Berlin, Germany model WILOW159-WIFI-HI-INC-30B) set to a recording frequency of 50 Hz. The sensor had an accuracy of $\pm 0.02^\circ$, temperature compensation, and wi-fi communication. Two triaxial accelerometers (Gulf Coast Data Concepts LLC, Waveland, MS, USA, model X2-2), with a theoretical accuracy of $\pm 0.0044^\circ$ and equipped with a built-in datalogger, were used to monitor guyline anchors and tiebacks.

In Block 2 and 3, cable tensile forces (expressed in kN) applied to guyline anchors and tailholds were monitored using purpose-built pre-calibrated load cells. These load cells were connected to data loggers (Campbell Scientific, Logan, United States, model CR1000x) set to record at a frequency of 100 Hz. The load cells were installed between anchor straps and haul-back blocks at the tailholds, and between guylines and anchor straps (or guyline extension) at the guyline anchors (Fig. 4). The distance between the point of application of the tensile force (i.e., position of

the anchor straps/guyline extension on the anchors) and the ground was measured to estimate the lever arm of such forces and derive the applied moment. While the analysis of the moment should refer to the pivotal point of the produced rotation, the identification of such point is not feasible in operational conditions (large displacement, i.e., near to failure conditions are required as reported by Marchi et al. 2022), and the hinge is generally assumed at soil level in most pulling tests (Peltola et al. 2000).

Data concerning cable tensile forces, time study, machine positions, and ground information were initially processed, synchronized, and analysed by means of GIS software and R-scripts, following established procedures (e.g., Mologni et al. 2021a). The following anchor stability analysis was conducted in Matlab[®] environment, extending the methodological approach described in Marchi et al. (2021).

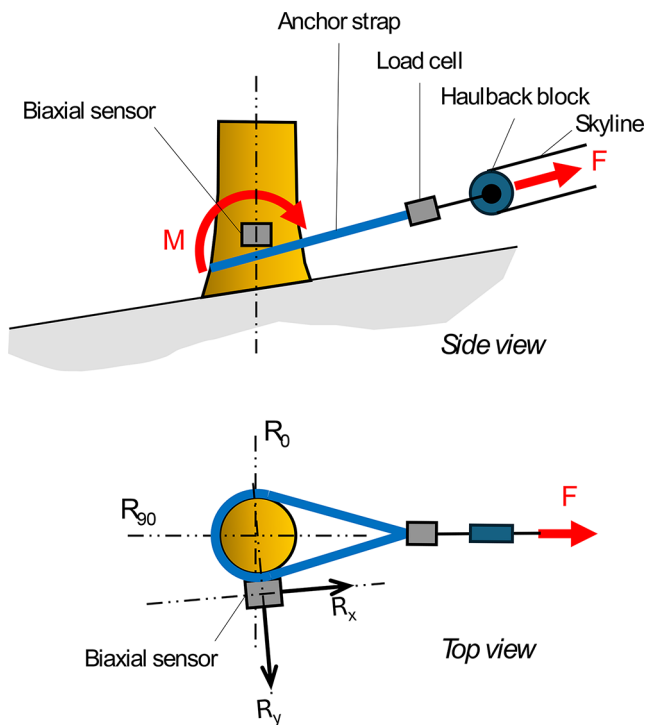


Fig. 4 Schematic representation of the sensor layout and the main measured scalar quantities

Anchor stability analysis

Root-plate rotations and stiffness calculation

Installation inaccuracies and unknown preferential axis root growth (Lundstrom et al. 2007; Marchi et al. 2021) may provide an offset between the axes of the local coordinate system of the biaxial sensor (R_x , R_y) with the axes over which the maximum and minimum rotations are expected, respectively the axis parallel (R_0) and perpendicular (R_{90}) to the direction of the pulling force.

In Block 1, the anchor rotation parallel to the pulling direction R_0 was simply derived from the recorded sensor rotations (R_x , R_y) following the same methodology described in Marchi et al. (2021), namely $R_0 = (R_x^2 + R_y^2)^{1/2}$. This approach, satisfactory when measuring large rotations and directions (e.g., unstable anchors or destructive tests) is suitable to overcome the unavailability of cable tensile force data. On the opposite, when dealing with very small rotations (e.g., sturdy trees or stumps showing values root-plate rotation (R) $< 0.5^\circ$), limited offsets in the measured axes alignment may lead to large errors when comparing those values with theoretical rotation limits. Linking rotations to forces and moments through the stiffness computation becomes a crucial aspect that allows to overcome the question whether the observed rotations are actually generated by the pulling cable or not. In this context, in Block 2 and

3, where applied forces and moments were available, the azimuthal offset (ΔR) necessary to rotate R_x and R_y , was calculated with a more complex but robust iterative procedure aimed to find the axis orientation which minimized the average stiffness of the anchor. Stiffness relates root-plate rotations (expressed in degrees, deg or $^\circ$) to the moment causing them (expressed in kNm), where the latter is the product between a force (in kN) and its lever arm (in m). Here, the lever arm was calculated starting from the orthogonal distance between the point of application of the forces and the ground, corrected by the slope of the cable (see Marchi et al. 2022 for details about employed equations and additional schematics). The slope of the cable was computed for each anchor by the inclination of the theoretical chord derived from the relative difference in altitude (derived from the digital elevation model) between the selected anchor and the cable yarders, accounting for the height of the boom of the cable yarders. Finally, the calculation of the azimuthal offset (ΔR) was performed via the following steps:

1. For each work cycle, calculation of stiffness (K_i , referred also as elastic stiffness) as the slope of the linear regression between applied moment and root-plate rotation data and its corresponding coefficients of determination (r^2_i).
2. Evaluation of a mean stiffness K and mean r^2 among all calculated K_i and r^2_i .
3. Progressive rotation of the axes with azimuthal increments ΔR of 10° and, within each iteration, recalculation of stiffness K_i per cycle and their mean values.
4. Identification of the decisive ΔR from visual analysis of local minima in the mean stiffness K and local maxima in its related r^2 (Fig. 5). This can be translated in the angle for which the same amount of force generates the maximum rotations (local minima of stiffness) with the clearest data output (local maxima of r^2).

Computation of cyclic loading effects

The mechanical response of each anchor was first analysed by deriving maximum values of root-plate rotations not only over the whole monitored time (R_{max}), but within each work cycle ($R_{i, max}$) and performing a regression analysis over the number of cycles (i.e., a sort of temporal evolution of anchor stiffness). A deeper analysis of cyclic loading effect was then applied on data from Blocks 2 and 3, given the availability of cable tensile force measurements and related moments applied to the anchors. This novel protocol for cyclic loading effect monitoring can be summarized in two additional steps:

Fig. 5 Variation of average stiffness and r^2 according to increasing ΔR for anchor GA3.1

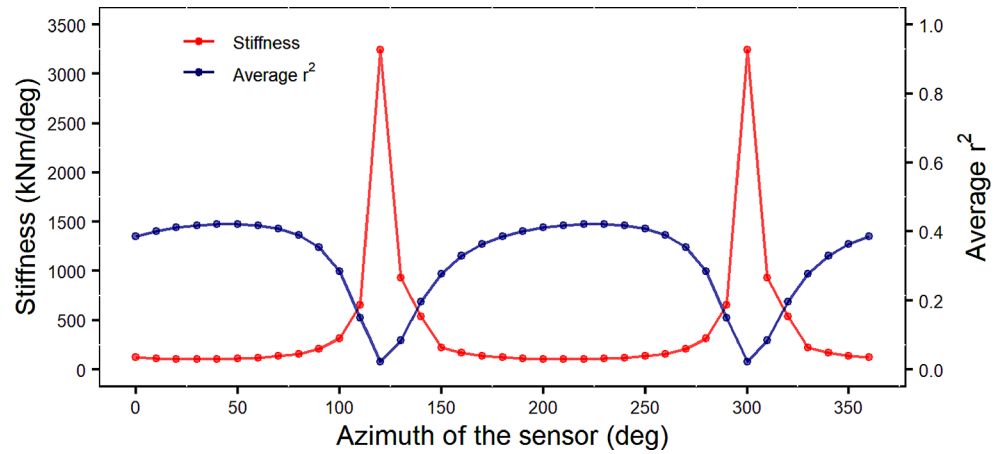


Table 3 Tailhold, tieback and guyline anchor main mechanical parameters recorded

Cable road ID	Anchor ID	Observed time (H)	PMH ₁₅ (h)	Work cycles (n.)	F _{max} (kN)	Slope (deg)	Lever arm (m)	R _{max} (deg)
C1.1	TH1.1	6.82	5.80	59	-	5.7	-	10.97
	TB1.1.1	6.82	5.80	59	-	-	-	6.73
C1.2	TH1.2	4.61	3.53	60	-	3.2	-	1.68
	TB1.2.1	4.61	3.53	60	-	-	-	0.22
	TB1.2.2	4.61	3.53	60	-	-	-	0.19
C2.1	TH2.1	2.72	2.55	22	160.5	-13.6	0.29	1.20
	GA2.3	3.48	2.70	23	63.6	-24.1	0.27	0.15
C2.2	TH2.2	2.32	2.12	21	150.3	-16.4	0.29	0.29
	GA2.3	1.64	1.62	16	104.1	-24.1	0.27	0.15
C2.3	TH2.3	1.43	1.27	16	169.3	-18.8	0.28	0.43
	GA2.3	1.57	1.07	8	100.7	-24.1	0.27	0.04
C2.4	TH2.4	4.05	3.64	28	163.7	-22.6	0.46	2.63
	GA2.3	7.08	5.51	44	90.8	-24.1	0.27	0.17
C2.5	TH2.5	4.66	3.68	30	209.4	-26.3	0.27	0.37
	GA2.3	5.01	3.68	30	105.6	-24.1	0.27	0.11
C3.1	TH3.1	0.06	0.00	0	NA	-18.2	0.28	NA
C3.2	TH3.2	1.79	1.34	48	245.0	-17.3	0.29	0.71
	TB3.2.1	1.79	1.34	48	-	-	-	0.04
C3.3	TH3.3	1.64	1.25	54	277.2	-22.3	0.28	1.59
	TB3.3.1	1.64	1.25	54	-	-	-	0.20
C3.4	TH3.4	1.95	1.16	43	273.1	-21.2	0.28	0.39
	TB3.4.1	1.95	1.16	43	-	-	-	0.06
C3.5	GA3.1	4.07	1.32	49	181.8	-14.1	0.10	0.34
	TH3.5	2.60	1.99	92	220.1	-22.9	0.28	1.31
	TB3.5.1	0.68	0.56	28	-	-	-	0.26
C3.6	GA3.1	3.06	1.99	92	172.7	-14.1	0.10	0.37
	TH3.6	4.02	1.96	60	200	-23.5	0.27	0.46
C3.7	GA3.3	3.75	2.45	62	148.0	-14.1	0.10	0.34
	TH3.7	4.50	2.07	73	210.2	-23.5	0.27	1.63
C3.8	TB3.7.1	3.74	1.45	43	-	-	-	0.15
	GA3.3	4.22	2.08	72	167.6	-14.1	0.10	0.07
	TH3.8	2.20	1.54	57	201.9	-23.4	0.27	0.19
	GA3.3	2.73	1.86	68	238.9	-14.1	0.10	0.12

5. Transformation of the one-cycle stiffness K_i into non-dimensional terms, achieved by dividing it by its maximum value ($K_{i,max}$) recorded on the same anchor over the whole monitored time (i.e., stiffness ratio). This approach also facilitates a more comprehensive understanding of overall stability relative to initial conditions and enables a more robust comparison of cyclic loading effects across different anchors.
6. Regression of the ratio $K_i/K_{i,max}$ over number of cycles, and derivation of the slope coefficient. This coefficient, expressed as a percentage, was designated as the damage index (I_D). The damage index quantifies the accumulated “damage” within each cycle, indicating the progression of stiffness degradation over time.

Comparison with theoretical rotation limits

Best-practice guidelines and general predictive models of tree stability recommend a direct comparison of equivalent moment values between destructive pulling tests and anchor stability surveys. To accomplish this, the linear regression models of the applied moment at failure (M_{peak}) over stem volume predictors, such as $DBH^2 \times H$ and DBH^3 , published by Byrne and Mitchell (2007) could be used at first. However, the approach proposed by Marchi et al. (2019) uses regression models of rotation at failure (R_{Mpeak}) over the same predictors and could provide better results, especially noting that tiebacks modify the actual force exerted on the tree leading to unprecise quantification of the real forces and moments applied to the tree. Therefore, values of R_{Mpeak} (i.e., failure conditions) measured from the tilt sensors set at the base (height from soil of about 30 cm) were extrapolated from the original moment vs. rotation curves available from Byrne and Mitchell (2007) and smoothed according to the approach reported in Lundström et al. (2007) i.e., using a locally weighted, quadratic, polynomial smooth algorithm with a fixed window span equal to 10% of the data points. Then, linear models of R_{Mpeak} and M_{peak} were used to compute the theoretical failure values of rotation $R_{Mpeak,th}$ and moment $M_{peak,th}$ for selected tailholds (i.e., limited to the case of standing trees with the same tree species of the pulling tests). Comparisons between observed values and the theoretical limits were finally performed and expressed as the two safety factors: $S_R = R_{max}/R_{Mpeak,th}$ and $S_M = M_{max}/M_{peak,th}$.

Results

A conspicuous dataset could be derived from all the surveys, registering anchor base rotations from a total of 1522 work cycles of which 1224 work cycles included also tensions measurements. In detail, tailholds were monitored for a total of 45.4 h, covering 33.9 PMH₁₅ and 663 work cycles, spread over 12 workdays and three case studies (Table 3). The majority of the work cycles (427) were recorded during grapple yarding operations in Block 3, accounting for a total of 11.3 PMH₁₅. Observations in Block 1 and 2 covered a similar amount of work cycles (119 and 117 cycles, respectively), but accounted for a different amount of productive time (9.3 and 13.3 PMH₁₅, respectively) due to the different yarding solutions adopted. In Block 1, where the observations focused on root-plate rotations only, a grapple carriage was used for the first 30 work cycles on cable road C1.1, while chokers for the remaining 89 cycles. Operations in Block 2 relied exclusively on the use of mechanical carriage and chokers, slowing down the operations. While the grant average cycle time was 3.07 min/cycle, average cycle time per block varied from 1.59 (Block 3) to 6.80 (Block 2) min/cycle. Tieback, when installed as support of tailholds, were monitored partially simultaneously with the tailholds. The observations of tiebacks were limited to two case studies (being absent in Block 2) and interested a total of 21.2 h, 15.1 PMH₁₅ and 335 work cycles. Observations on guyline anchors were limited to Block 2 and 3 interested a total of 10 workdays, 36.6 h, 24.7 PMH₁₅ and 483 work cycles. Again, most of the work cycles (361) were collected during grapple yarding operations in Block 3, monitoring 141 cycles on GA3.1 and 220 cycles on GA3.3, for a total of 10.0 PMH₁₅. A single guyline anchor in Block 2 was monitored for 14.7 PMH₁₅ but only 122 work cycles, as the used of chokers reduced the hourly number of cycles. Average cycle time calculated for guyline anchors showed slightly different values compared to the tailhold analysis as the monitored work cycles were only partially overlapping. Overall average cycle duration observed on guyline anchors was 2.98 min/cycle, ranging from 1.64 (Block 3) to 7.20 (Block 2) min/cycle.

Root-plate rotations and cable tensile forces

Direct field measurements of anchor response to applied force focus on root-plate rotations and cable tensile forces. Peak values of maximum root-plate rotations per cycle (R_{max}) recorded at the various natural anchors ranged from 0.19° to 10.97° for tailholds, from 0.05° to 6.73° for tiebacks, and from 0.09° to 0.52° for guyline anchors. The highest values of R_{max} at tailholds and tiebacks were recorded in Block 1, on cable road C1.1, and were linked to an anchor system just

next to failure. Excluding those anchors, peak R_{max} values would have been 2.63° for tailholds and 0.26° for tiebacks. Overall, tailholds were the anchor type typically showing the highest rotation, while tiebacks and guyline anchors reported much more limited values.

R_{max} exceeded 0.5° in 11 anchors, nine of them were tailholds, while one was the tieback in cable road C1.1 and one the guyline anchor GA3.1. $R_{i,max}$ exceeding 0.5° was recorded in 94 work cycles for tailholds, distributed in all three case studies, but 59 of which were linked to the observations on cable road C1.1. Only 26 work cycles reported $R_{i,max}$ exceeding 0.5° for tiebacks, all of them in cable road C1.1.

The range of maximum root-plate rotations recorded per cycle ($R_{i,max}$) was comparable between stump and anchor trees, even if the maximum absolute values were recorded on stumps. Similarly, no significant effect on range and maximum values was observed in rotations only by the anchor size or the fact that the anchor was support or not by tiebacks.

Measurement of applied forces and related moments and stiffness were limited to Block 2 and 3. Maximum tensile forces recorded per cycle ($F_{i,max}$) at tailholds ranged between 34 and 277 kN. The highest tensile forces were normally recorded in Block 3, were pulling forces generated by the Madill 122 reached or exceeded 200 kN in all cable roads and 34 work cycles. These forces were frequently higher for cable road C3.2, C3.3, and C3.4 because their yarding direction was not perpendicular to the ground slope (Fig. 3) and the skyline deflection was limited as much as possible to permit upward lift on the logs, leading to increased tensile forces for similar payload and conditions. The Washington 78SL used in Block 2 generated forces at the tailholds that exceeded 200 kN only in two work cycles of cable road C2.5 due to the need of reducing skyline deflection because of need of negotiating obstacles along the ground profile (Fig. 6), while the other four cable roads reported peak

values of maximum tensile forces recorded per cycle (F_{max}) limited to 150–169 kN.

Cable tensile forces measured at guyline anchors were generally more limited than those recorded at the tailholds, as the payload was partially spread over two or three different guylines. Absolute maximum F_{max} at guyline anchor was 239 kN recorded on GA3.3. F_{max} on the other guyline anchor monitored in the same block (GA3.1) reached a maximum of 182 kN, and in Block 2, F_{max} reached a maximum of 106 kN. However, the progressive changes in the cable geometry layout led to a progressive variation in F_{max} values over consecutive roads (Fig. 7). While at guyline anchor GA3.1, progressive cable road change led to increasing angles between skyline and monitored guyline and reduction in recorded F_{max} , the opposite was true for guyline anchor GA3.3. The progressive reduction of the skyline-guyline angle increased $F_{i,max}$ recorded at the guyline anchor, to the point that in cable road C3.8 it reached similar or higher values than those recorded at the tailhold.

A particular event of note was recorded during the monitoring of cable road C3.1. This cable road does not account for any work cycle and related $R_{i,max}$ or $F_{i,max}$ because its tailhold failed during the initial set up, before any actual yarding operation (Fig. 8). Tailhold TH3.1 was a 38-cm DBH western hemlock, secured with a tieback to a large old-growth stump with a synthetic sling. During the first loading, the tree showed a linear elastic response up to a pulling force of 100 kN. However, at about 115 kN, the tree started to rotate progressively, up to a critical rotation of 7.1° . Tensile force in the skyline was immediately released bringing the force down to 20 kN, registering a residual rotation of 2.6° . The tieback strap at the tailhold was then shifted upward to 1 m from the ground to increase the leverage effect of the stabilizing force. However, at the beginning of the second pull the tree leaned forward critically upon reaching just 40 kN of force, showing a compromised stability and was therefore substituted with a different anchor (TH3.2).

Fig. 6 Maximum cable tensile force (F_{max}) and root-plate rotation (R_{max}) per work cycle at tailholds of Block 2 and Block 3

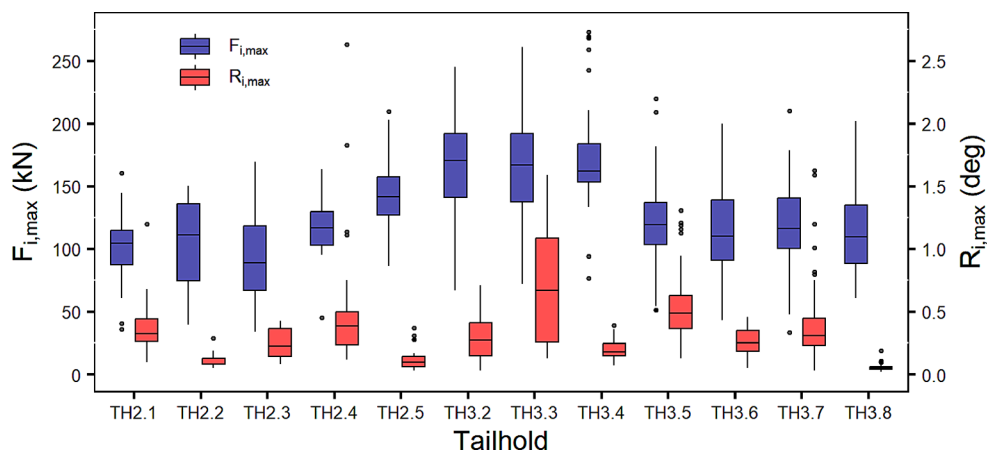


Fig. 7 Maximum cable tensile force ($F_{i,max}$) and root-plate rotation ($R_{i,max}$) per work cycle at guyline anchors of Block 2 and Block 3

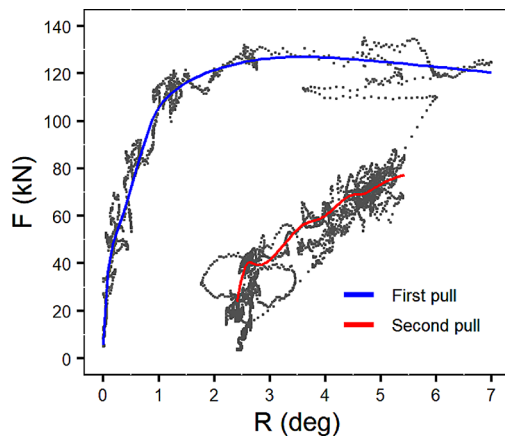
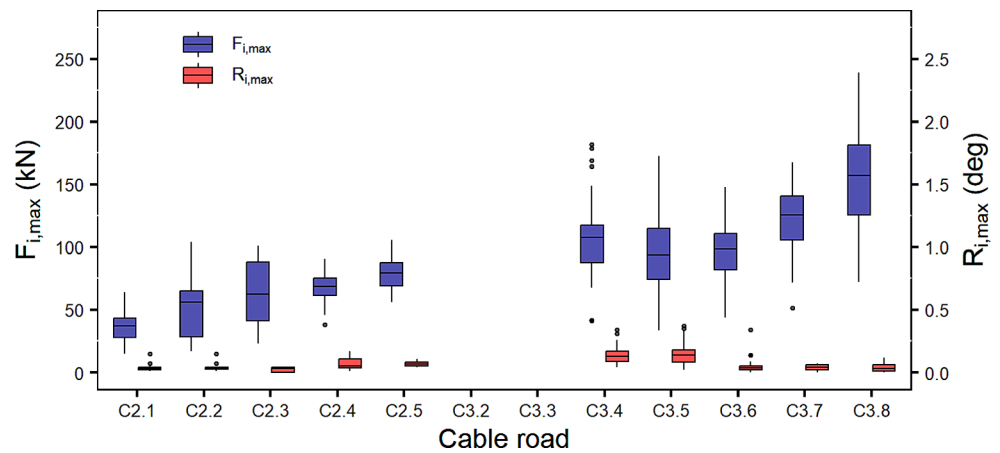


Fig. 8 Root plate rotation (R) vs. applied cable tensile force (F) at tailhold TH3.1

Response due to cyclic loads

Rotations vs. number of work cycles

The effects of repeated cyclic loading may be observed as an increasing trend in the magnitude of the peak rotation over the number of work cycles n . Therefore, a simple linear regression of the maximum root plate rotation per cycle ($R_{i,max}$) over the number of cycles was performed on all the 25 monitored anchors presenting data (Table 4). However, failure of normality and homoscedasticity assumptions in the residuals for some anchors led to the logarithmic transformation of the dependent variable R_{max} before reapplying the linear regression. This choice is supported by the non-linear response observed in the rotation range of these anchors, particularly in some tailholds. This transformation resulted in a better stabilisation of the variance of the residuals. Log-transformation required filtering sporadic negative values of $R_{i,max}$ which occurred in 36 cycles from the total of 1522 that were removed only from guylines GA2.3 and GA3.3. The analysis showed that 14 (56%) anchors showed a direct relationship between $R_{i,max}$ and n , but only five of

them (20%), including TH1.1, TH3.2, TH3.3, and TH3.6, showed a positive correlation ($r^2 > 0.5$). The remaining anchors returned poorer, null, or insignificant correlation between $R_{i,max}$ and n .

A good example of the different response in peak rotation's magnitude over the number of load cycles was recorded in the preliminary observations carried out in Block 1. In cable road C1.2, tailhold and tiebacks showed an almost null slope of the linear regression (Fig. 9a). The opposite was recorded for cable road C1.1, where both the tailhold and the related tieback employed showed a progressive deterioration of the anchor stability, suggesting a relevant impact of cyclic loading (Fig. 9b). In such case, $R_{i,max}$ at the tailhold started at about $1.5\text{--}3^\circ$ and increased up to 7.5° approaching the end of the first workday (cycle #39), further increasing up to almost 11° during the second day. Similarly, $R_{i,max}$ of the related tieback (TB1.1.1) started at about 0.3° and exceeded 1.5° by the end of the first day, reaching a peak of 6.7° on the last day of observations. It is important to note that a heavy load yarded during cycle #34 created a peak on the rotation and a sudden irreversible damage to tieback TB1.1.1 (Fig. 10), which led to increased $R_{i,max}$ at both tailhold and tieback and strongly reduced the overall stability of the anchoring system. Because of the compromised stability of the tailhold and tieback, the payload of the last few work cycles was reduced, and consecutively $R_{i,max}$ was reduced.

Stiffness vs. load cycles

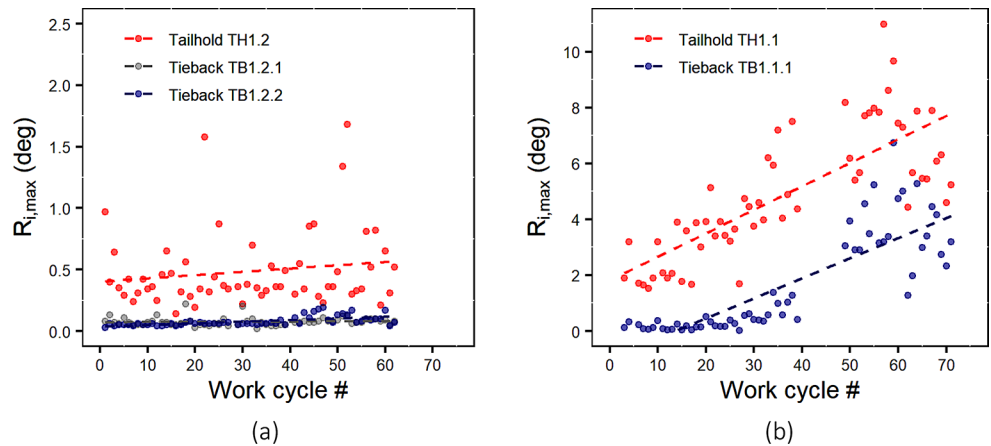
The safe and reliable behaviour of an anchor over repeated loading must also ensure that the initial relationship between applied moment and root plate rotation is maintained. If the opposite is the case, the anchor is experiencing cyclic loading drawbacks. Continuous evaluation of stiffness is a valuable approach to confirm that reported increases in rotations are not a consequence of an increase in applied moments but are the result of an impairment of the tree / stump anchoring

Table 4 $R_{i,max}$ vs. number of cycles: regression slope coefficients and goodness of fit output

Cable road ID	Anchor ID	Observations	r^2	Slope Estimate	Std. Error	p -value	F-value
C1.1	TH1.1	59	0.601	0.084	0.0091	< 0.001*	5.438
	TB1.1.1	59	0.699	0.072	0.0062	< 0.001*	-3.284
C1.2	TH1.2	60	0.025	0.003	0.0022	0.223	5.072
	TB1.2.1	60	0.004	0.001	0.0003	0.616	4.795
	TB1.2.2	60	0.391	0.000	0.0022	< 0.001*	8.141
C2.1	TH2.1	22	0.082	-0.010	0.0077	0.195	4.870
C2.2	TH2.2	21	0.052	0.002	0.0017	0.319	4.455
C2.3	TH2.3	16	0.111	-0.009	0.0067	0.207	4.914
C2.4	TH2.4	28	0.113	0.021	0.0117	0.080	1.077
C2.5	TH2.5	30	0.267	0.005	0.0015	0.004*	1.760
C2.1 to C2.5	GA2.3	122	0.066	0.000	0.0003	0.004*	4.860
C3.1	TH3.1	-	-	-	-	-	-
C3.2	TH3.2	48	0.716	0.010	0.0009	< 0.001*	1.557
	TB3.2.1	48	0.001	< 0.001	0.0001	0.876	11.928
C3.3	TH3.3	54	0.521	0.019	0.0026	< 0.001*	1.716
	TB3.3.1	54	0.017	< 0.001	0.0003	0.338	5.298
C3.4	TH3.4	43	0.001	< 0.001	0.0009	0.873	8.594
	TB3.4.1	43	0.194	< 0.001	0.0002	0.003*	1.908
C3.5	TH3.5	92	0.124	0.003	0.0009	< 0.001*	7.615
	TB3.5.1	28	0.231	0.004	0.0013	0.010*	2.439
C3.6	TH3.6	60	0.665	0.004	0.0004	< 0.001*	7.806
C3.7	TH3.7	73	0.108	-0.004	0.0015	0.005*	8.513
	TB3.7.1	43	0.407	< 0.001	0.0002	< 0.001*	13.624
C3.8	TH3.8	57	0.244	< 0.001	0.0002	< 0.001*	4.430
C3.1 to C3.5	GA3.1	245	0.124	< 0.001	0.0002	< 0.001*	9.310
C3.6 to C3.8	GA3.3	261	0.004	< 0.001	0.0001	0.299	9.366

*Significant at $p = 0.05$

Fig. 9 Maximum root-plate rotation ($R_{i,max}$) per cycle of tailhold and tiebacks of cable road C1.2 **a** and C1.1 **b**



capacity. In (Marchi et al. 2021) data from at least 4 h of PMH_{15} , resulting in at least 27 work cycles, was used as a threshold to look for evidence of cyclic effects. In order to be consistent with this previous work while investigating a yarding system with a higher productivity, the following analysis was performed on anchors for which direct measurements of cable tensions and root plate rotations were available for at least 25 work cycles. This included 12 anchors, nine tailholds and three guyline anchors, or five

freshly-cut stumps and seven trees, distributed between Block 2 and Block 3.

Half of the selected anchors (five trees and one stump) showed some evidence of cyclic loading effects with a negative value of I_D (Table 5) but only tree tailholds proved to be statistically significant (p -value < 0.05). Tailhold TH3.2 provides a clear example of a decreasing stiffness per cycle K_i (Fig. 11a), where rotation associated with similar peak tensile forces increased from about 0.1° during the initial

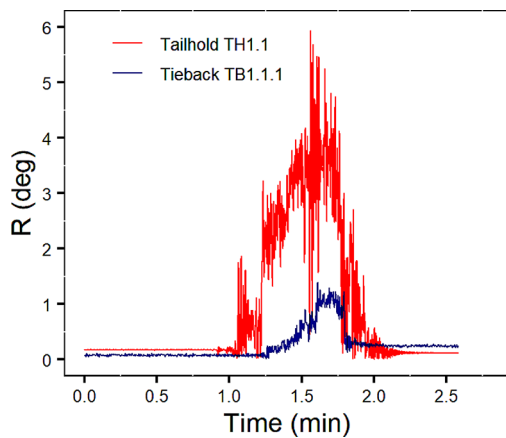


Fig. 10 Evidence of irreversible damage occurred to tieback TB1.1.1 at load cycle #34

cycles, up to 0.5° after about 50 work cycles. From the cross comparison between the variation of $K_i/K_{i,max}$ and the corresponding r_i^2 values over the number of cycles (Fig. 12a) emerges the progressive reduction of K_i and the parallel increasing r_i^2 , with the first parameter reducing to about a third of the initial values, and the latter shifting from ~ 0.2 up to ~ 0.8 . A similar response (negative I_D and increasing r_i^2 trend) was recorded for tailhold TH3.6. Analysis on

TH3.3, TH3.7 and GA2.3 returned a limited dependency of the stiffness over number of cycles. In this case, analysis of the residuals did not show any issues for TH3.2, TH3.6 and TH3.7 provided that a some outliers were removed and could be recognized as work cycles with a particularly low force magnitude.

The six remaining anchors (four stumps and two trees) did not show negative cyclic loading effects. Three stumps (TH2.4, GA3.1, GA3.3) and one tree (TH2.5) showed an almost constant response over time, with $I_D < \pm 0.1\%$. Two tailholds, one tree (TH3.4) and one stump (TH3.5), reported limited but positive values of I_D ($> 0.1\%$), suggesting an apparent progressive increment of stiffness over cyclic loading. Figure 11b shows an example of that for tailhold TH3.5, where no sign of the variation of the calculated indexes were detected, and were an increased scattering of the later cycles produced a small but positive increase of K_i (Fig. 12b). In this regard, it must be considered that tailhold TH3.5 was monitored in two workdays, separated by four days because of the heavy snowfall and a weekend in between. Stational conditions (e.g., soil conditions) might have been slightly different for the two observed days and might have had an impact on the limited differences in the recorded stiffness.

Fig. 11 Root plate rotation and moment at tailhold TH3.2 a and TH3.5 b. Colored lines show the one-cycle stiffness, from the first (blue) to the last cycle (red)

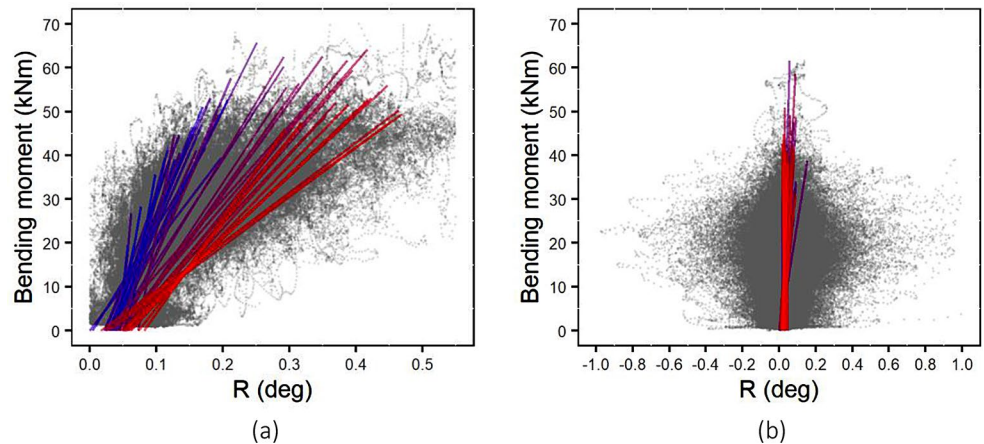


Fig. 12 Non-dimensional stiffness $K_i / K_{i,max}$ and corresponding r_i^2 plotted over work cycle # at tailhold TH3.2 a and TH3.5 b. Slope of the dashed lines represent the damage index (blue) and determination index (red)

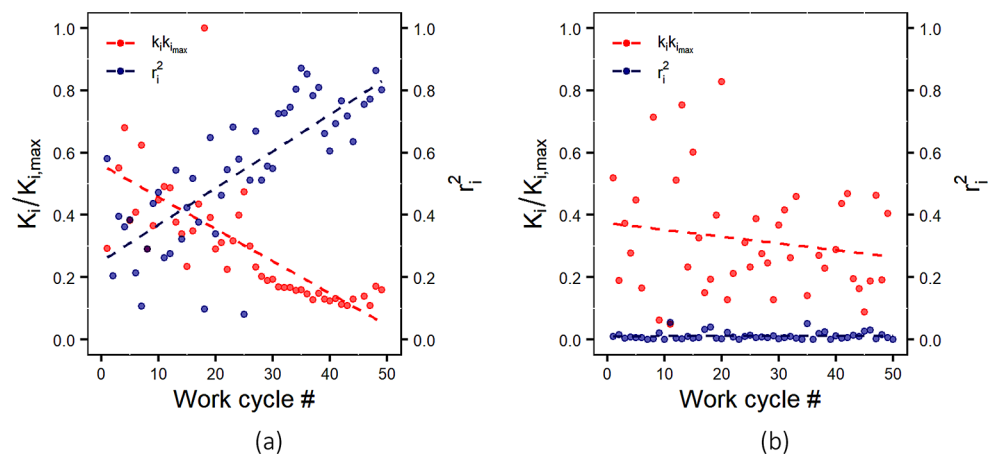


Table 5 $K_i / K_{i,max}$ vs. number of cycles: regression slope coefficients (I_D) and goodness of fit output of the estimate

Anchor ID	Observations	Average K_i	Average r^2_i	DoF	I_D (%)	r^2	p -value	F-value
TH2.4	28	1447	0.07	25	-0.41	0.03	0.407	0.710
TH2.5	30	1435	0.15	28	0.09	0.00	0.855	0.034
TH3.2	48	294	0.56	44	-1.29	0.69	<0.001*	97.899
TH3.3	54	216	0.26	52	-0.26	0.14	0.005*	8.727
TH3.4	43	1297	0.08	41	-0.12	0.01	0.591	0.293
TH3.5	92	1930	0.01	87	0.05	0.01	0.441	0.599
TH3.6	60	195	0.59	58	-0.39	0.37	<0.001*	33.412
TH3.7	73	413	0.25	69	-0.41	0.18	<0.001*	15.492
TH3.8	57	1987	0.09	53	-0.20	0.02	0.285	1.165
GA2.3	121	2132	0.09	119	-0.04	0.02	0.128	2.355
GA3.1	141	1661	0.03	134	0.07	0.03	0.034*	4.594
GA3.3	202	1077	0.27	200	0.12	0.23	<0.001*	59.158

* Significant at $p=0.05$

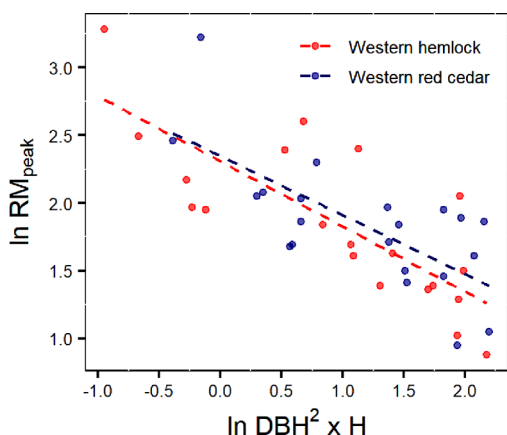


Fig. 13 Log-linear regression obtained from pulling test data with (Byrne and Mitchell 2007)

Response against theoretical failure limits

Safety factors are normally used to limit the allowable stress applied to certain elements (e.g., wire ropes in cable yarding) to guarantee a sufficient threshold to the working load with respect to their failure limits. Safety factors depend on several variables as likelihood of damages to people and machines, level of precision of the manufacturing process, level of maintenance etc. Up to now, no specific guidelines explicit in detail safety factors to the field of tree stability, and even more to the case of cable logging. In this work,

the evaluation of safety factor was therefore based on comparison between R_{max} and theoretical failure values derived from reference pulling tests performed in the proximity of Block 1 and Block 3, on soils having comparable characteristics and for the same tree species, namely Western hemlock and Western red cedar.

R_{Mpeak} was positively related to the allometric stem volume predictor $DBH^2 \times H$ for both Western hemlock and Western red cedar with r^2 equal to 0.503 and 0.615, respectively (Fig. 13). Aggregating the two datasets, under the hypothesis that the two species provide a similar architecture of the root system and a consequent similar response, would result in a $r^2=0.560$. This outcome, allowed to predict a reasonable value of $R_{Mpeak,th}$ and consequent safety factor relative to the rotations S_R . For consistency, results had to be limited to the case of tailholds represented by Western hemlock standing trees and therefore could be performed for six tailholds (Table 6).

Tailhold TH3.1, TH 3.3 and TH3.7, as they showed sizes ($DBH^2 \times H$) in the range of the pulling test data (0.42–8.98 m³, corresponding to -0.87 to 2.19 after the logarithmic transformation), returned the lowest values: the model correctly captured the evidenced failure of tailhold TH3.1 ($S_R < 1$); tailholds TH3.3 and TH3.7 with S_R equal to 2.2 showed that the presence of tiebacks provided a good restraint and secured them a sufficient reserve of rotation capacity. The remaining three tailholds, TH2.5, TH3.4 and TH3.6, fall out

Table 6 Theoretical values at failure and related safety factors

Anchor ID	$DBH^2 \times H$ (m ³)	R_{max} (°)	$R_{Mpeak, th}$ (°)	S_R	M_{max} (kNm)	$M_{peak, th}$ (kNm)	S_M
TH2.5	19.16	0.37	2.43	6.6	62.8	374.5	5.9
TH3.1	4.33	7.10	4.96	0.7	40.5	84.7	2.1
TH3.3	8.76	1.59	3.54	2.2	138.6	171.2	1.2
TH3.4	11.92	0.53	3.05	5.8	81.9	233.0	2.8
TH3.6	14.14	0.46	2.81	6.1	60.0	276.4	4.6
TH3.7	8.71	1.63	3.55	2.2	63.1	170.4	2.7

of the range of validity of the model, whilst simply extending the linearity of the model would show very conservative results with S_R value up to 6.6. Only for demonstration purposes, Table 6 includes the theoretical safety factor based on moment values S_M . Results shows not conservative (i.e., reduced or absent safety limits) values for all cases, failing in predicting the safety of tailhold TH3.1 whereas suggesting close to failure conditions for tailhold TH3.3.

Discussions

This study presents unique evidence of stability assessment of trees and stumps used as natural anchors across coastal British Columbia in ordinary cable yarding operations employing running skyline configurations. The research focused on observing root-plated rotations of selected anchors, examined the effect of cable tensile forces and related moments on such rotations, and proposes a new method for quantifying the temporal evolution of their impact on the anchor responses. To do so, a total aggregated monitoring of 103 h of root-plate rotations and 80 h of cable tensile forces were monitored over 12 workdays and three case studies.

Anchor stability assessment rely on the analysis of propensity of failure due to uprooting (i.e., overturning failure) because the rigging cables were set at ground level and failure to stem breakage can be disregarded. The observed data was investigated according to several methodologies: (i) comparison of absolute values of rotations with known elastic limits of trees; (ii) correlation between the maximum rotation per load cycle vs. number of load cycles; (iii) correlation between the stiffness per load cycle vs. number of load cycles; (iv) comparison of rotation values with respect to predictive linear models based on tree pulling tests data.

At the operational level, the literature shows that root plate rotations lower than 0.25° ensure a total elastic response of the tree root system i.e., irreversible damages to the root system are precluded (Wessolly and Erb 1998). These limits appear to be extended up to 0.5° for shallowly rooted trees (Lundström et al. 2007; Sagi et al. 2019) and even more for stumps (Marchi et al. 2022).

Observations of standing trees monitored in this study showed that large-size trees (DBH larger than 70 cm), with or without tiebacks, have limited root plate rotations, with R_{max} limited to 0.45° (e.g., TH2.2, TH2.3, TH2.5, TH3.8, GA2.3), and therefore could have been considered stable and safe according to this approach. Trees with DBH ranging from 55 to 70 cm (e.g., TH3.4, TH3.6, TH3.10) showed R_{max} within the threshold of 0.50° , but with a higher contribution to the stability given by the tiebacks. Smaller sized trees, e.g., tailholds TH3.3 and TH3.7, showed R_{max} well

beyond the recommended threshold of $0.25\text{--}0.50^\circ$, and the presence of the tiebacks proved to be strictly necessary to keep them working elastically and prevent their failure due to uprooting. The failure of the smallest tree observed during the trials, tailhold TH3.1, provided evidence that even the use of a tiebacks may not be sufficient to stabilize a tree with a relatively small DBH. In this regard, it is also noticeable that the presence of tiebacks on small size tailhold trees (e.g., TH3.3, TH3.6 and TH3.7) has never been sufficient to increase the overall stiffness up to the levels demonstrated by the larger trees, at least in the observed case of synthetic slings without twisting.

Observations linked to stumps, particularly for tailholds TH2.1 and TH2.4, showed elastic responses with peak root plate rotations up to 1.3° . This suggests that safety limit of $0.25\text{--}0.50^\circ$ assumed for trees may be too conservative for stumps, and a higher limit may be accepted, as found in Marchi et al. (2022). This is a direct consequence of the absence of the compression given by the tree self-weight which reduces the overall exhibited stiffness of the root system. Tieback TB1.1.1, although demonstrating a significantly impaired stability, has been successfully used at peak rotations up to 4° , even if this is absolutely not recommended considering the hazard that an imminent uprooting may represent.

Overall, guyline anchors were the most stable anchors observed in the study. Guyline anchors are the most important anchors in a cable yarding operation because they directly support the yarder stability. The contractors carefully selected suitable trees/stumps to be used for these anchors, shifting toward the use of equipment in case of limited tree/stump sizes. On the other hand, tailholds were selected mostly based on their location to locate the cable system on proper location, with more tolerance on limited tree size, if needed.

Numeric evidence in the study confirmed that the stability of an anchor can change significantly over time and the effects of subsequent load cycles may affect its response as they produce increases of peak base rotations (see also O'Sullivan and Ritchie 1993). Cyclic loading analysis is particularly relevant because, while the lack of stability of an anchor may be clearly identified at the first pulls (e.g., tailhold TH3.1), field evidence suggested that initially stable conditions may change rapidly due to its repeated and continued use, with rotations increasing proportionally with the number of applied cyclic loading (e.g., TH1.1 and TB1.1.1 or TH3.2 and TH3.6). The lack of long-term or cyclic loading data and consolidated methods of analysis, forced the development of the novel and robust approach based on a linearization analysis of applied moment and rotations. The proposed method should be preferred from an engineering point of view as it ensures calculations are always performed

within the maximum force range, is independent from resonance/vibration phenomena affecting rotation readings, and automatically detects irreversible rotations.

Degradation of the anchoring capacity was analyzed via the evaluation of a damage index I_D , in line with consolidated approaches applied in structural engineering to detect damages to structures caused by failure of materials and already applied to model the response of the root system of trees (Yang et al. 2014, 2020). According to this method, half of the selected anchors provided signs of cyclic loading effects, while an almost null response was recorded for the remaining ones. Although absolute values of stiffness might be partially impacted by variations in the estimates of the lever arms, relative stiffness observations within individual anchors provides solid evidence for cyclic loading effect analysis. In comparison, Marchi et al. (2021) found significant damage indexes for 11 out of 15 selected anchors observed for standing skyline cable systems in typical European conditions. Note that cyclic loading analysis might have a different significance between European standing skyline systems (where anchors can be used for multiple days or, sometimes, weeks) and cable yarding based on running skyline systems (where the combination of short cable roads and short/quick work cycles linked to the use of grapple carriages provided a much quicker but shorter evolution of the anchor's response).

Cross comparisons between the two approaches, i.e., rotation vs. load cycles and the stiffness vs. load cycles, provided that the latter may be extremely useful to confirm or not stability impairments detected by the first one. The progressive increase of maximum rotations for tailholds TH3.2 and TH3.6 was confirmed by the negative damage index I_D . In other words, the increasing rotations were proven to be not a consequence of increasing applied forces and momentums but a real amplification of base rotations. The stiffness approach was proven also to be a valuable tool to analyse apparent compromised conditions returned by the rotation-only approach. In detail, tailhold TH3.3, reported a significant response after the sole analysis of rotations (p -value = 0.005 and $r^2 = 0.52$), whereas evaluation of the stiffness trend was able to confirm the cyclic response reduction stiffness did occur to the anchor ($I_D = -0.23$ and $r^2 = 0.14$) but in a much limited form. Furthermore, the cyclic response measured as a function of $R_{i,max}$ of cycle number showed that what was detected as a cyclic loading effect on TH2.5, TH3.5, and GA3.1 was indeed due to increased tensile forces and not to a decrease anchoring capacity. In conclusion, the rotation vs. load cycles approach does provide an initial guess and is convenient at least when tensile forces are not known, but it's the stiffness vs. load cycle methodology that can actually shed more light on the behavior of the anchor. It must also be highlighted that the

requirement about the simultaneous measurement of tensile forces and rotations reduced, in this study, the sample number of anchors to 12 (including the requisite of at least 25 consecutive work cycles) with respect to the 25 (analysed with the rotation only approach), (Table 4 vs. Table 5).

Root plate rotation values at failure of shallowly rooted conifers have been collected through dedicated tree pulling tests in coastal British Columbia (Byrne 2005). These limit values are estimated to be between 3° and 15° and are inversely proportional to the tree size. With the application of the approach described in Marchi et al. (2019) and using preliminary analysis from the pulling test data available by Byrne and Mitchell (2007), the observed root plate rotations could be compared with the expected values of rotation at failure. The consistency of the comparison is further supported by two additional facts: (i) the dataset is limited to western hemlock ($n=20$) and western red-cedar ($n=21$), namely the same tree species observed in this study; (ii) partial overlapping between the $DBH^2 \times H$ parameter derived for the investigated trees (0.42 – 8.98 m³) and the one of the datasets (4.33 – 19.16 m³). From the evaluation of the safety factor, TH3.1 operated over its critical range (and indeed it failed). TH3.3 and TH3.7 were employed with a safety factor of 2.2, while TH2.5 and TH3.6 operated with a safety factor higher than six against overturning. It was also demonstrated how comparing equivalent moment would have shown different and not conservative (in terms of safety) results. It is worth noting, that this procedure shows how the integration of results from dedicated pulling tests can be used for defining best practices and safety limits to be used in operational conditions. On the opposite, this methodology requires that a great variety of tree species, soil conditions, type of anchor (full tree or stump) is investigated by means of specific tree pulling tests to be applicable at a large scale.

Conclusions

Stability assessment protocol of trees and stumps used as anchors in cable yarding operations, initially developed for standing skyline systems, was tested with swing yarders in running skyline configuration. The current work gave numeric evidence of three tailholds being almost pulled from the ground during yarding operations (one at the first pull during the cable road set up and two after about 40 work cycles) confirming that high magnitudes of the forces generated by cable yarders and the lack of large diameter trees and stumps may lead to a potentially high risk of anchor failure.

Evolution of the maximum base rotation calculated within each work cycle provide a preliminary outcome of

the anchor's overall cyclic response, however the computation of the mechanical stiffness does provide better clarity ensuring that increased rotations are a consequence of stability reduction and not an increase of pulling force.

Analyses on the response due to cyclic loads showed that in six out of twelve situations, the anchors demonstrated a decreasing stiffness trend over time showing how an initially apparent stable condition may negatively evolve due to repeated loads and the consequent accumulation of damages at the root-soil interface.

The comparison between theoretical failure limits and actual anchor rotations could be considered also a valid approach as measurement of tensile forces may be avoided, however a considerable amount of species-specific data from tree pulling tests is required.

The work also showed that the multitude of rigging configuration employed in cable yarding operations and the high number of variables that intervene in the mechanical response of each anchor do not allow a simple generalization of the anchoring capacity of natural anchors. Therefore, the development of a dedicated monitoring solution equipped with an inclinometer and a portable single-board computer able to run an algorithm following the proposed method of analysis (thus producing a case-by-case stability assessment procedure) and transmit wirelessly the outcomes to the yarding operator appears to be the most recommendable solution.

Further research should concentrate in the validation of the proposed technique in different environments, soil and ground conditions and with different yarding equipment and crews. Additional knowledge could be also obtained with tree/stump pulling tests of tree species and dimensions not covered by the available research works.

The authors declare that they have no known competing financial interests or personal relationships that could have appeared to influence the work reported in this paper.

Supplementary Information The online version contains supplementary material available at <https://doi.org/10.1007/s10342-024-01714-9>.

Acknowledgements The authors would like to thank FPInnovations, Skytech Yarding, Fall River Logging, and Wheeler Equipment for their support in the data collection.

Author contributions L.M. and O.M. collected the field data, performed the analyses and wrote the main manuscript text; O.M. prepared figures. K.B. supervised partial data analysis; S.G. and D.R. conceived and co-planned the research. All authors reviewed the manuscript.

Funding Open access funding provided by Università degli Studi di Padova within the CRUI-CARE Agreement. This research was performed within the Agritech National Research Center and received funding from the European Union Next-GenerationEU (PIANO NAZIONALE DI RIPRESA E RESILIENZA (PNRR) – MISSIONE 4

COMPONENTE 2, INVESTIMENTO 1.4 – D.D. 1032 17/06/2022, CN00000022).

Open access funding provided by Università degli Studi di Padova within the CRUI-CARE Agreement.

Data availability Datasets are available on request.

Declarations

Not applicable.

Competing interests The authors declare no competing interests.

Open Access This article is licensed under a Creative Commons Attribution 4.0 International License, which permits use, sharing, adaptation, distribution and reproduction in any medium or format, as long as you give appropriate credit to the original author(s) and the source, provide a link to the Creative Commons licence, and indicate if changes were made. The images or other third party material in this article are included in the article's Creative Commons licence, unless indicated otherwise in a credit line to the material. If material is not included in the article's Creative Commons licence and your intended use is not permitted by statutory regulation or exceeds the permitted use, you will need to obtain permission directly from the copyright holder. To view a copy of this licence, visit <http://creativecommons.org/licenses/by/4.0/>.

References

- Amishev D, Evanson T, Raymond K (2009) Felling and bunching on steep terrain - A review of the literature. Future Forest Research Limited, Rotorua, New Zealand
- Belart F, Leshchinsky B, Wimer J (2020) Deadman anchoring design for cable logging: a new approach. *Can J for Res* 50:342–357. <https://doi.org/10.1139/cjfr-2019-0338>
- Byrne KE (2005) Critical turning moments and drag equations for British Columbia conifers. University of British Columbia
- Byrne KE, Mitchell SJ (2007) Overturning resistance of western redcedar and western hemlock in mixed-species stands in coastal British Columbia. *Can J for Res* 37:931–939. <https://doi.org/10.1139/X06-291>
- Cavalli R (2012) Prospects of research on cable logging in forest engineering community. *Croatian J for Eng* 33:339–356
- Harrill H, Visser R (2016) Skyline Tension Behavior of Rigging Configurations Used in New Zealand Cable Logging. In: Proceedings of the 2016 Council on Forest Engineering Annual Meeting. Vancouver, Canada
- Heinimann HR (1999) Ground-based harvesting technologies for steep slopes. In: Proc. Int. Mountain Logging and 10th Pacific Northwest Skyline Symp. Corvallis, OR
- Holzfeind T, Visser R, Chung W et al (2020) Development and Benefits of Winch-Assist Harvesting. *Current Forestry Reports* 2020 6:3 6:201–209. <https://doi.org/10.1007/S40725-020-00121-8>
- Leshchinsky B, Sessions J, Wimer J, Clauson M (2016) Designing Mobile anchors to yield: a tension relief system for tail anchoring. *Croatian J for Eng* 37:269–278
- Liley W (1983) Cable logging handbook. New Zealand Logging Industry Research Assn., Rotorua N.Z
- Lundstrom T, Jonas T, Stockli V, Ammann W (2007) Anchorage of mature conifers: resistive turning moment, root-soil plate geometry and root growth orientation. *Tree Physiol* 27:1217–1227. <https://doi.org/10.1093/treephys/27.9.1217>
- Lundström T, Jonsson MJ, Kalberer M (2007) The root-soil system of Norway spruce subjected to turning moment: resistance

- as a function of rotation. *Plant Soil* 300:35–49. <https://doi.org/10.1007/s11104-007-9386-2>
- Mancuso A, Belart F, Leshchinsky B (2018) Operative loading in cable yarding systems: field observations of static and dynamic tensions in mobile anchor systems. *Can J for Res* 48:1406–1410. <https://doi.org/10.1139/cjfr-2018-0219>
- Marchi L, Grigolato S, Mologni O et al (2018) State of the art on the use of trees as supports and anchors in forest operations. *Forests* 9:467. <https://doi.org/10.3390/f9080467>
- Marchi L, Mologni O, Trutalli D et al (2019) Safety assessment of trees used as anchors in cable-supported tree harvesting based on experimental observations. *Biosyst Eng* 186:71–82. <https://doi.org/10.1016/j.biosystemseng.2019.06.022>
- Marchi L, Mologni O, Grigolato S, Cavalli R (2020) Evaluation on the Stability of Tree used as anchors in Cable Yarding operations: a preliminary Test based on low-cost MEMS sensors. Lecture notes in Civil Engineering. Springer, Cham, pp 473–479
- Marchi L, Trutalli D, Mologni O et al (2021) Mechanical response of natural anchors in cable logging. *Int J for Eng* 32:29–42. <https://doi.org/10.1080/14942119.2021.1826882>
- Marchi L, Costa M, Grigolato S, Lingua E (2022) Overturning resistance of large diameter Norway spruce (*Picea abies* (L.) Karst) on sloped conditions. *Ecol Manage* 524:120531. <https://doi.org/10.1016/j.foreco.2022.120531>
- Mologni O, Lyons CK, Zambon G et al (2019) Skyline tensile force monitoring of mobile tower yarders operating in the Italian Alps. *Eur J Res* 138:847–862. <https://doi.org/10.1007/s10342-019-01207-0>
- Mologni O, Lyons CK, Marchi L et al (2021a) Assessment of cable tensile forces in active winch-assist harvesting using an anchor machine configuration. *Eur J Res*. <https://doi.org/10.1007/s10342-020-01347-8>
- Mologni O, Marchi L, Lyons CK et al (2021b) Skyline tensile forces in cable logging: field observations vs. software calculations. *Croatian J for Eng* 42:227–243. <https://doi.org/10.5552/crojfe.2021.722>
- O’Sullivan MF, Ritchie RM (1993) Tree stability in relation to cyclic loading. *Forestry* 66:69–82. <https://doi.org/10.1093/forestry/66.1.69>
- Omule SAY, Kozak A (1989) Stump and Breast Height Diameter Tables for British Columbia Tree Species FRDA report 062
- OR-OSHA (2010) Yarding and loading handbook. Oregon Occupational Safety and Health Division, Salem, OR (USA)
- Parker SPS (2001) Evaluation of Stump Strength for Temporary Forest Road Design. In: International Mountain Logging and 11th Pacific Northwest Skyline Symposium. Seattle, WA, pp 136–144
- Parker S (2002) Preliminary evaluation of stump strength for the design of temporary forest roads
- Peltola HM, Kellomäki S, Hassinen A, Granander M (2000) Mechanical stability of scots pine, Norway spruce and birch: an analysis of tree-pulling experiments in Finland. *Ecol Manage* 135:143–153. [https://doi.org/10.1016/S0378-1127\(00\)00306-6](https://doi.org/10.1016/S0378-1127(00)00306-6)
- Pestal E (1961) Seilbahnen und seilkrane für holz un materialtransport. Georg Fromme & Co, Wien
- Pyles MR (1987) Structural properties of Second-Growth Douglas-Fir logging spars. *Trans ASAE* 30:0065–0069. <https://doi.org/10.13031/2013.30403>
- Pyles MR, Stoupa J (1987) Load-carrying capacity of second-growth Douglas-fir stump anchors. *West J Appl for* 2:77–80. <https://doi.org/10.1093/wjaf/2.3.77>
- Pyles MR, Anderson JW, Stafford SG (1991) Capacity of second-growth Douglas-fir and western hemlock stump anchors for Cable Logging. *J for Eng* 3:29–37. <https://doi.org/10.1080/08435243.1991.10702631>
- Safe Work Australia (2013) Guide to managing risks in Cable Logging. Canberra, Australia
- Sagi P, Newson T, Miller C, Mitchell S (2019) Stem and root system response of a Norway spruce tree (*Picea abies* L.) under static loading. *Forestry: Int J for Res* 92:460–472. <https://doi.org/10.1093/forestry/cpz042>
- Samsel I (1985) Winch and cable systems. Springer Netherlands, Dordrecht
- Stoupa J (1984) Behavior and load carrying capacity of stump anchors. Oregon State University
- Toupin RC, Pyles MR, Tuor B, Tour B (1985) Modelling and testing two-stump anchors. LIRA Tech Release ISSN 0111–4743 7:1–4
- Tsioras PA, Rottensteiner C, Stampfer K (2011) Analysis of accidents during cable yarding operations in Austria 1998–2008. *Croatian J for Eng* 32:549–560
- Visser R, Stampfer K (2015) Expanding ground-based harvesting onto steep terrain: a review. *Croatian J for Engineering: J Theory Application Forestry Eng* 36:321–331
- Wessolly L, Erb M (1998) Handbuch Der Baumstatik Und Baumkontrolle [Manual of Tree Statics and Tree Inspection]. Patzer, Berlin, Germany
- Work Safe BC (2006) Cable yarding systems handbook. Second edition. Workers’ Compensation Board of British Columbia, Vancouver
- Yang M, Défossez P, Danjon F, Fourcaud T (2014) Tree stability under wind: simulating uprooting with root breakage using a finite element method. *Ann Bot* 114:695–709. <https://doi.org/10.1093/aob/mcu122>
- Yang M, Défossez P, Dupont S (2020) A root-to-foilage tree dynamic model for gusty winds during windstorm conditions. *Agric Meteorol* 287. <https://doi.org/10.1016/j.agrformet.2020.107949>

Publisher’s Note Springer Nature remains neutral with regard to jurisdictional claims in published maps and institutional affiliations.